JCTC Journal of Chemical Theory and Computation

Proton Transfer Dynamics in Crystalline Maleic Acid from Molecular Dynamics Calculations

Przemyslaw D. Dopieralski,*,† Zdzislaw Latajka,† and Ivar Olovsson‡

University of Wroclaw, Faculty of Chemistry, 14 Joliot-Curie Str. 50-383 Wroclaw, Poland, and Department of Materials Chemistry, Ångström Laboratory, SE-751 21 Uppsala, Sweden

Received February 9, 2010

Abstract: The crystal structure of maleic acid, the cis conformer of HOOC−CH═CH−COOH has been investigated by Car−Parrinello molecular dynamics (CPMD) and path integral molecular dynamics (PIMD) simulations. The interesting feature of this compound, compared to the trans conformer, fumaric acid, is that both intra- and intermolecular hydrogen bonds are present. CPMD simulations at 100 K indicate that the energy barrier height for proton transfer is too high for thermal jumps over the barrier in both the intra- and intermolecular hydrogen bonds. Dynamics at 295 K reveal that the occupancy ratio of the proton distribution in both the intra- and intermolecular hydrogen bonds is 0.96/0.04. The time lag between the proton transfers in the intra- and intermolecular hydrogen bonds is in the range of 2−9 fs. This is slightly shorter than the time lag obtained previously for fumaric acid, where only intermolecular hydrogen bonds are present. It is also interesting to notice that in most cases the proton transfer process starts in the intramolecular hydrogen bond and subsequently follows in the intermolecular hydrogen bond. Vibrational spectra of the investigated system and its deuterated analogs HOOC−CH═CH−COOD and DOOC−CH═CH−COOD have been calculated and compared with experimental data.

Introduction

Carboxylic acids are typical examples of molecular systems with double hydrogen bonds. Several experimental[1−5] as well as theoretical[6−9] studies of the proton transfer dynamics in such systems have been done recently. But there is still a lack of experimental and theoretical data in the literature for the proton transfer dynamics in dicarboxylic acids. Among the dicarboxylic acids, the cis and trans conformers of butenedioic acid, HOOC−CH═CH−COOH, maleic and fumaric acid, respectively, play a very important role. The physical properties of maleic acid are very different from those of fumaric acid, so it is of interest to study this system and to compare it with our previous results on crystalline fumaric acid.[10] Maleic acid is used in organic synthesis, in the polymer industry, and in oil conservation.[11−14] It is also an inhibitor of fumarate dehydrogenase. Salts of maleic acid are also used in the pharmaceutical industry for drug preparation. Polymorphism is of crucial importance in this context as different crystal structures of the same material may have markedly different physicochemical properties.

Although maleic acid has a wide range of applications and is of biological significance, the literature data are rather limited. The trans isomer, fumaric acid, forms infinite chains of double hydrogen bonds (H-bonds), whereas the cis isomer, maleic acid, forms infinite chains of single H-bonds, as one of the protons is involved in an intramolecular H-bond (Figure 1). The O···O distances, 2.64 Å for the intermolecular and 2.50 Å for the intramolecular H-bond,[15] are shorter than the O···O distance in fumaric acid, 2.67 Å,[16] which suggests that it may be possible to observe similar proton transfer processes as seen in fumaric acid.[10] In fumaric acid, benzoic acid,[17] and $KHCO_3$,[18] the protons are disordered, and the occupation of two possible positions varies with temperature. The situation in maleic acid is complicated as there are two different types of H-bonds. In this particular situation, theoretical calculations are able to provide informa-

* Corresponding author e-mail: mclar@elrond.chem.uni.wroc.pl.
† University of Wroclaw.
‡ Ångström Laboratory.

10.1021/ct100078w
Published on Web 04/14/2010

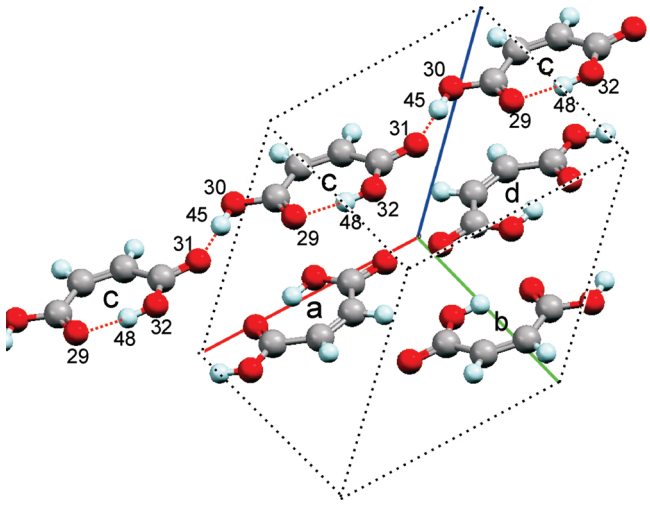

Figure 1. Crystal structure of maleic acid.

tion about the occupation ratio by integration of the distribution functions. In previous X-ray studies, there are no reports of experimentally determined occupation ratios, therefore our investigations are initially restricted to the atomic positions determined by the X-rays structure. The spectroscopic study of isolated maleic acid was essentially limited to the matrix-isolated structure.[19]

The proton transfer reaction in proteins and in solution has been studied extensively.[20−22] In the literature, there are also numerous theoretical papers which deal with double proton transfer, most of which involve the isolated formic acid dimer.[23] The real turning point in study of formic acid dimer dynamics was work by Miura et al.,[6] where authors investigated double proton transfer reaction. Two types of ab initio simulations were carried out: one type of nuclei were treated classically, while in the other, they were quantized via the path integral. In several recent papers, the double proton transfer (DPT) reaction in the cyclic dimer of chloroacetic acid has also been studied using Car−Parrinello molecular dynamics (CPMD) and path integral molecular dynamics (PIMD) techniques, cf. Durlak et al.[9] According to these studies the proton transfers in the isolated system are asynchronous (the two protons do not pass the midpoints of their respective H-bonds at exactly the same time). The two-step mechanism proposed by Ushiyama and Takatsuka for DPT[7] was consistent with the CPMD results. These authors also agree that there is a coupling between the O−H stretching motions and the low-frequency vibrational modes.[2,3,24−26] In the present work, we are taking these studies one step further. To the best of our knowledge intra- and intermolecular H-bond couplings obtained by the CPMD and PIMD methods in the "solid state" have not been compared previously.

Calculations

This work involves CPMD and PIMD calculations of crystalline maleic acid based on the code CPMD,[27] version 3.11.1.[28] The crystal data from the X-ray study by James and Williams[15] have been selected as starting point (cf. also refs 29 and 30). The crystal is monoclinic ($P2_1/c$) with cell dimensions $a = 7.473$, $b = 10.098$, $c = 7.627$ Å, and $\beta = 123.59°$ with four formula units in the unit cell ($Z = 4$).[15] The unit cell of the crystal contains four maleic acid molecules, and each of them forms separate chains (in Figure 1 the content of one unit cell is shown, but the H-bonds in only one chain are illustrated for clarity). The molecules in the unit cell have been optimized with periodic boundary conditions (PBC), and the proton transfer has been studied at 100 and 295 K. A kinetic energy cutoff of 100 Ry was used for the electron plane-wave basis. Troullier and Martins pseudopotentials[31] and Perdew et al. exchange and correlation functional[32] were applied. To control the temperature of the system, the Nosé-Hoover chain thermostat[33,34] was set for the whole system at a target temperature of 100 and 295 K and a coupling frequency of 3000 cm^{-1}.

In the PIMD case, a separate thermostat was used for each degree of freedom.[35] We used time steps of 3 au. The PIMD simulation[36−38] explores the quantum behavior of both the nuclear and electronic degrees of freedom. It maps the problem of a quantum particle onto one of a classical ring polymer model with beads that interact through temperature- and mass-dependent spring forces. Such mapping is known in the literature as quantum-classical isomorphism.[39−41] The path integral simulations in the present study used eight beads and normal mode variable transformation.[38] Eight beads were used in our previous study on fumaric acid[10] and thus proved that such a number of beads is appropriate for the studied system. Dynamics runs of around 20 ps were performed for the crystalline maleic acid. A simulation with a box size of four unit cells, which we employed for fumaric acid[10] and $KHCO_3$[42] was not performed. The size and number of molecules inside one unit cell of maleic acid was deemed to be sufficient.

To study the proton transfer process, we introduce the reaction coordinate δ, defined as the difference between the r_{O-H} and $r_{H\cdots O}$ bond lengths. We use the same procedure to calculate the reaction coordinate for the intra- and the intermolecular H-bonds.

Vibrational spectra have been generated using the program by Forbert,[43] which calculates the spectrum using the inverse fast Fourier transform of the classical autocorrelation function of the total dipole moment, including all contributions—nuclear and electronic. The so-called high-temperature (or harmonic) quantum correction factors to the classical line shape functions were used to approximate the true quantum line shape function and thus the IR spectra.[44] This method is found to work well for anharmonic vibrational spectra and H-bonded systems.[45−48] The visual molecular dynamics program, VMD,[49] has been used for data visualization.

The applicability of density functional theory (DFT)-based methods to describe H-bonded systems depends on the nature of the interaction (these methods are known to have deficiencies in accounting for dispersion interactions).[50] The strong H-bonds in the present system are mainly dominated by electrostatic interactions,[51,52] which supports our choice of the computational methodology. Furthermore, it is important to note that the accuracy of the potential energy surface in Car−Parrinello simulations is determined by the exchange and correlation functionals used. In the CPMD studies of the acetic acid dimer in the gas phase, we have

Table 1. Selected Average Bond Distances (Å) in Crystalline Maleic Acid[a]

		crystal				
		CPMD	CPMD	CPMD	PIMD8	
	bond	opt.	100 K	295 K	295 K	expt[15]
c	O−H (32−48)	1.04	1.05	1.08 (1.03)	1.12 (1.07)	0.91
	O···H (29−48)	1.46	1.47	1.45 (1.48)	1.39 (1.41)	1.59
	O···O (29−32)	2.50	2.51	2.51	2.48	2.50
	O−H (30−45)	1.04	1.04	1.08 (1.03)	1.09 (1.05)	0.98
	O···H (31−45)	1.53	1.55	1.54 (1.53)	1.48 (1.49)	1.66
	O···O (30−31)	2.57	2.58	2.61	2.55	2.64

[a] PIMD8 - Path Integral with 8 beads; data in parentheses are the most probable values. CPMD opt: data from geometry optimization with PBC; most probable values: maximum value of the distribution function for the studied bond; the numbers in parentheses in the column "bond" refer to the atoms numbering in Figure 1.

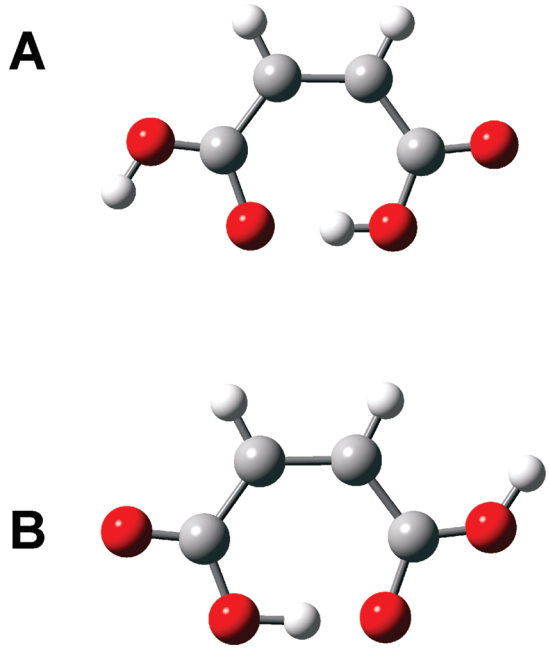

Figure 2. Two conformers studied in present work: (A) the most stable conformer and (B) the second conformer observed in our simulation. The illustrated structures differ by a 180° rotation of the −OH group.

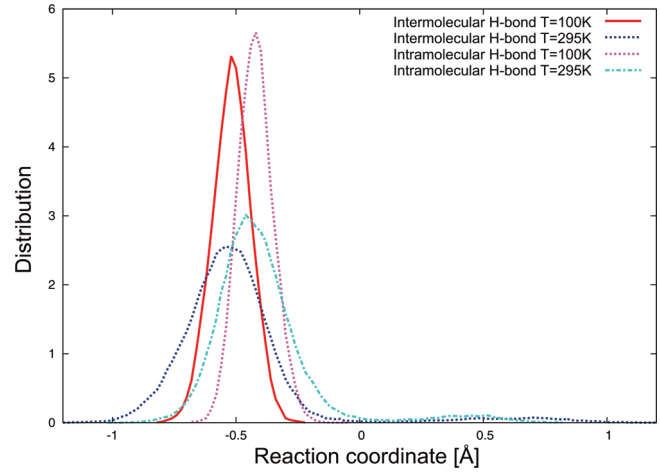

Figure 3. Distribution function (δ distribution) from CPMD at temperatures 100 and 295 K for the intra- and intermolecular H-bonds. Reaction coordinate (δ) is defined as the difference between $r_{O32-H48}$ and $r_{H48-O29}$ bond lengths for the intramolecular H-bond and as the difference between $r_{O30-H45}$ − $r_{H45-O31}$ bond lengths for the intermolecular H-bond.

shown that underestimation of the barrier height for proton transfer employing the DFT formalism is approximately compensated by neglecting the zero-point vibrational contribution in the simulations.[9]

Results and Discussion

Structural Parameters. Average bond lengths of the CPMD-optimized structure are compared with the results from the PIMD calculations and the X-ray study[15] in Table 1. Data are only shown for one maleic acid molecule. Bond lengths for other maleic acid molecules in the unit cell do not differ more than 0.01 Å (for CPMD at 100 K). For CPMD and PIMD simulations at 295 K, the differences are larger but still do not exceed 0.04 Å. It is worth pointing out that the conformer of maleic acid shown in Figure 2A was found by Macoas et al.[19] in IR matrix isolation and computational studies to be the most stable in the case of the isolated molecule, and this conformer is also present in the crystalline state. However, during the dynamics simulation, the conformer in Figure 2B was also observed. The energy gap between this conformer and the most stable one (Figure 2A) was predicted by Macoas et al. to be approximately 5.9 kcal/mol (in the case of the isolated system) at the B3LYP/6-31G(d,p) level. Figure 3 shows the difference between the intra- and intermolecular H-bond distribution functions at the two temperatures from the CPMD simulations. At 100 K, no population is observed around a reaction coordinate value of +0.5 Å, which corresponds to a situation where the proton in both the intra- and intermolecular H-bonds has been transferred. When the temperature is increased to 295 K, the distribution becomes broader. The question now arises whether there is a possibility that proton transfer may take place in only one of the two bonds and not in the second? In our case, we did not observe such a situation. For the different molecules in the same chain, something close to a collective mechanism, like in a Grotthuss model,[53,54] was observed. From the present simulations, we may conclude that the proton transfers in the four chains are independent of each other (cf. Figure 1). It is possible that when more than one cell is included in the simulations, new features will appear, but a long enough simulation with at least four unit cells is at present too expensive. This is one of possible future lines of investigations. The proton behavior in crystalline maleic acid is

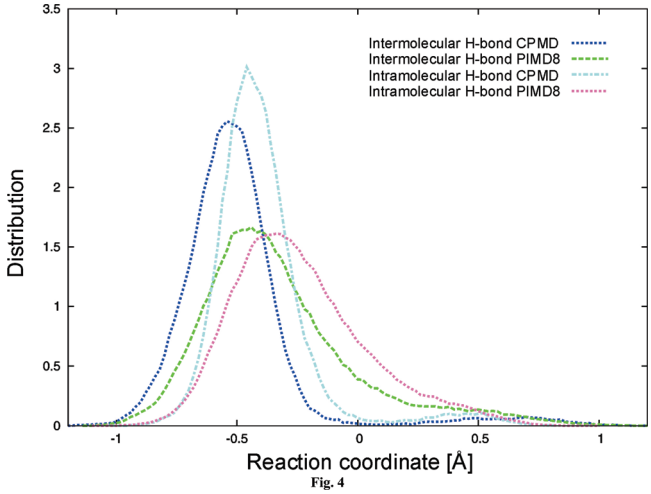

Figure 4. Distribution function at 295 K from CPMD and PIMD8 simulations for the intra- and intermolecular H-bonds.

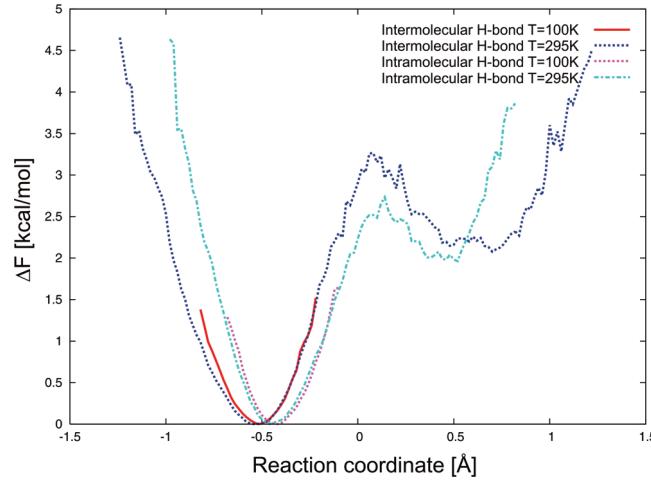

Figure 5. Single proton transfer free energy ΔF profile in crystalline maleic acid at 295 and 100 K from CPMD simulations for the intra- and intermolecular H-bonds.

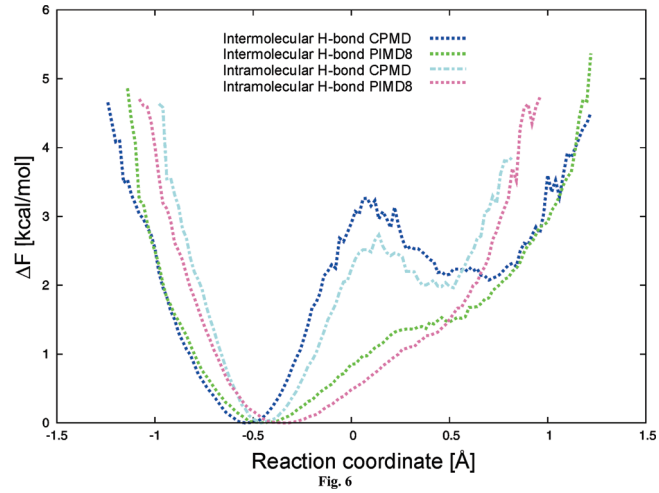

Figure 6. Single proton transfer free energy ΔF profile in crystalline maleic acid at 295 K from CPMD and PIMD8 simulations for the intra- and intermolecular H-bonds.

different depending on which of the standard CPMD and PIMD methods is used. No proton transfer is observed at 100 K using CPMD. PIMD calculations were not performed at 100 K as the strength of the H-bonds is about the same as in fumaric acid, and we accordingly expect similar results, namely that the thermal energy will be not sufficient to push protons across hydrogen bridges.

At 295 K proton transfer occurs with both the CPMD and PIMD methods (Figure 4), but in the PIMD simulation, proton transfers occur more often; the population at reaction coordinate = 0 Å is higher for PIMD than for that of CPMD. The next question is: do the protons transfer simultaneously or successively in the intra- and intermolecular H-bonds, and what is the time lag between the proton jumps? We performed a procedure similar to the one used by Ushiyama and Takatsuka,[7] where the relative coordinates n_1 and n_2 are defined to specify the position of the protons in the hydrogen bonds. Coordinate n_1 describes the proton in the intermolecular H-bond, and coordinate n_2 describes the proton in the intramolecular H-bond. When $n = 0.5$, the proton is exactly in the middle between the oxygen atoms. To the best of our knowledge, no one has earlier performed such a comparison.

$$\begin{aligned} n_1 &= r_{\mathrm{O31-H45}} \cos\theta_{\mathrm{O30-O31-H45}} / r_{\mathrm{O31-O30}} \\ n_2 &= r_{\mathrm{O32-H48}} \cos\theta_{\mathrm{O29-O32-H48}} / r_{\mathrm{O32-O29}} \end{aligned} \quad (1)$$

This procedure was applied for all four molecules in the unit cell. Analysis of these parameters shows that the proton transfers do not occur exactly simultaneously (with no time lag) or successively (with a large time lag between the transfers)—the observed situation is in between these two scenarios. However, based on the time lags, the proton transfers occur nearly simultaneously. The time series of the parameters n_1 and n_2 from the CPMD simulations allows us to calculate the time lag between the proton transfer in the intra- and intermolecular H-bonds. For the molecule marked (a) in Figure 1 there were four proton jumps with time lags 5, 7, 7, and 7 fs. For molecule (b) there were two proton transfers with time lags 2 and 9 fs. Four proton transfers were observed for molecule (c) with the time lags 8, 5, 7, and 5 fs. For molecule (d) no proton transfer was observed. The whole process of proton transfers in all of the molecules is completed within 40 fs. These values are influenced by the fact that simulations based on the DFT approach can underestimate the barrier, but an important factor is also the O···O distance. From an analysis of the n_1 and n_2, coordinates we may conclude that the intramolecular proton starts the process, and after that, the intermolecular proton is transferred. In the opposite proton transfer reaction, the intermolecular proton initiates the process. In almost all cases, such a situation was observed for all four molecules.

From our simulations of crystalline maleic acid, it is evident that conformer 2B is easily obtained by proton transfer. It was observed once for every 24 molecules of the most stable conformer 2A, as the CPMD occupancy ratio is 0.96/0.04. The free energy profiles obtained from each simulation type are shown in Figures 5 and 6. The profiles were calculated from the equation:

$$\Delta F = -kT\ln(P[\delta]) \quad (2)$$

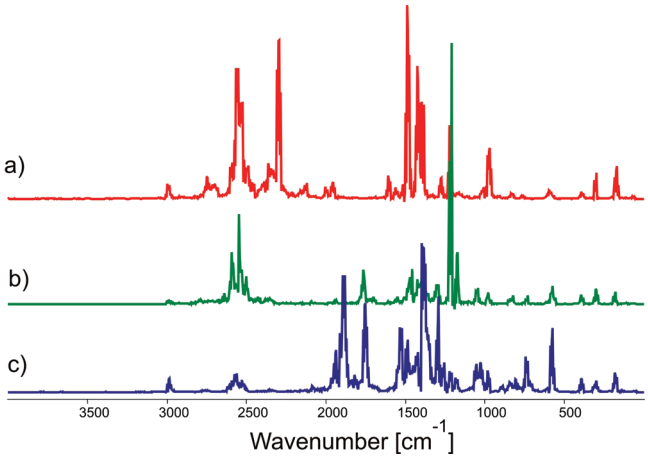

Figure 7. Comparison between theoretical spectra with selectively deuterated hydrogen atoms; upper (red) is without deuteration; middle (green) is only intramolecular H-bond deuterated; lower (blue) is with both intra- and intermolecular H-bonds deuterated. All spectra from autocorrelation of total dipole moments at 100 K.

Where k is the Boltzmann constant, T is the temperature, and $P[\delta]$ is the distribution profile for δ, and the reaction coordinate (δ) is defined as the difference $r_{O32-H48} - r_{H48-O29}$ between the bond lengths in the intramolecular H-bond and as $r_{O30-H45} - r_{H45-O31}$ in the intermolecular H-bond.

As demonstrated by the profiles in Figures 4 and 6, inclusion of quantum effects drastically changes the effective potential shape. The classical limit represented by the 295 K curve exhibits two minima separated by a free energy barrier of around 3.2 kcal/mol. Quantum effects introduced by the PIMD method tend to decrease the barrier. In the next step, we defined two new coordinates: $\rho_1 = r_{O32-H48} - r_{H48-O29}$ and $\rho_2 = r_{O29-O32}$ and then correlated them (data not shown). From this correlation, it was found that proton transfer occurs only when the O···O distance is shorter than the distance observed in the optimized structure. This is in agreement with our observations for fumaric acid and $KHCO_3$.[10,42] At 295 K, proton transfer occurs only when the O···O distance (for both the intra- and intermolecular H-bonds) is shorter than 2.5 Å.

Vibrational Spectra

The line shape of the O−H stretching modes of OH groups involved in H-bonds is very complex.[4] Many earlier attempts have been made to analyze the line shape of the O−H/O−D stretching band, mainly in acetic acid dimers in the liquid and gas phases.[55−57] Mechanisms such as Davydov splitting, Franck−Condon combinations with low frequency H-bond modes, multiple Fermi resonances,[58−60] hot bands, exchange tunnelling, predissociation, or breakdown of Born−Oppenheimer approximation have been considered.[55,56,58,59,61−63] Their relative influence on the line shape cannot be determined from the absorption spectrum alone.

In Figure 7, spectra are compared from three different CPMD simulations (from autocorrelation of total dipole moments) with different degrees of deuteration at 100 K. In the first case, only hydrogen in the intramolecular H-bond was deuterated, in the second case hydrogen in both the intra- and intermolecular H-bonds. According to the theoretical results, at 100 K the spectroscopic isotope effect ν_{O-H}/ν_{O-D} = 2556/1890 = 1.35 for the intermolecular H-bond and 2298/1762 = 1.30 for the intramolecular H-bond. A large isotopic ratio indicates a large anharmonicity in the H-bond. It is assumed that an isotopic ratio of the order of 1.3 is typical for medium to strong H-bonds.[64] The assignment of bands in the infrared spectrum for crystalline maleic acid is presented in Table 2.

Table 2. Bands Observed in the IR Spectrum of Crystalline Maleic Acid from CPMD Calculations at 100 K

	T = 100 K	
Band (cm^{-1})	H	D
O−H strech. inter.	2556	1890
O−H strech. intra.	2298	1762
O···O strech. inter.	173	184
O···O strech. intra.	308	299
C=O strech.	1487	1467
C−O strech.	1424, 1218	1303, 1218
C−O strech. intra.	1280	1303
C−H strech.	2995	2987
C=C strech.	1606	1554
C−C strech.	833	827

Here, the description of molecular vibrations was obtained from a classical approach to the nuclear motions, which is the basis of CPMD. Further studies of the vibrational character of maleic acid crystals require the use of a quantum approach to nuclear motion. There are approaches aimed at recovering at least some quantum effects from the CPMD trajectory at a small additional computational cost.[65,66] We would like, however, to remain at the classical level of describing nuclear motion. The main aim of our study is an analysis of the correlation between intra- and intermolecular events, and very accurate description of molecular vibrations is of secondary importance. Solving the multidimensional vibrational Schrödinger equation would be too costly for the purpose of this work.

A comparison between the theoretical spectrum of crystalline maleic acid and the experimental data in the spectral data base system (SDBS)[67] is shown in Figure 8 (the 295 K spectrum from the CPMD simulation with autocorrelation of total dipole moments is not shown here). In this spectrum, a broad absorption band is observed in the range 3100−1900 cm^{-1} due to the proton transfer process. A clearer spectrum was obtained from autocorrelating the velocities—but one must note that the intensities in this spectrum do not represent the true intensities, in contrast to the spectrum obtained by autocorrelating the total dipole moments. Nevertheless, from the spectrum at 295 K one can notice a broad absorption (OH stretching in the intra- and intermolecular bonds) in the range 3100−1900 cm^{-1} due to the proton transfer process. In order to obtain a more resolved spectrum, we have also used the data from the 100 K simulations, where proton transfer was not observed. In Figure 8B, we notice that the theoretical spectrum at 100 K differs significantly in the −OH stretching mode range in comparison with the experimental spectrum. Better agreement is achieved when we compare with the theoretical spectrum at 295 K (where proton transfer

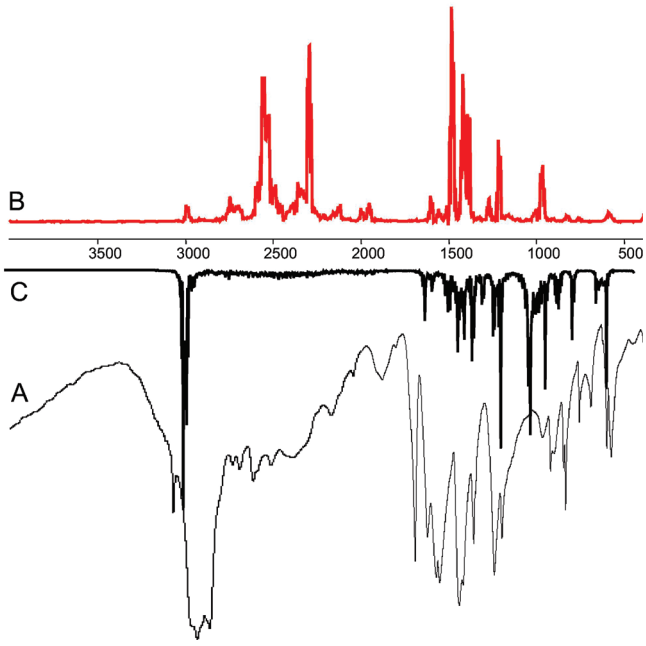

Figure 8. Comparison between experimental A (lower black, IR Nujol)[62] and theoretical spectra B (upper red): theoretical spectrum from dynamics with autocorrelation of total dipole moments at 100 K (no proton transfer) and C (middle black): from dynamics with autocorrelation of atomic velocities at 295 K (with proton transfer).

was observed), Figure 8C. This supports our earlier conclusions that proton transfer occurs at 295 K.

Conclusions

A less stable conformer 2B has been observed besides conformer 2A in our molecular dynamics simulations of crystalline maleic acid. The occupancy ratio (2A/2B) is around 0.96/0.04, which suggests that conformer 2B was observed once for every 24 molecules of the more stable conformer 2A. This ratio is quite small, and as the structure of 2B is not very different from 2A, it is probably very difficult to identify conformer 2B experimentally. Our calculations have shown that the whole proton transfer process starts in the intramolecular hydrogen bond (H-bond) and after that in the intermolecular H-bond. The opposite proton transfer process starts in the intermolecular H-bond. The stronger intramolecular H-bond may accordingly be considered as a switch, which makes the double proton transfer possible. But this is not true for the opposite process! The time gap between the proton transfers is in the range of 2−9 fs, which is more limited when compared to our previous observations in fumaric acid (1−24 fs)[10] and $KHCO_3$ (1−20 fs).[42] This limited range suggests that the proton motion in the intra- and intermolecular H-bonds has to be highly correlated and much more correlated than in the fumaric acid and $(HCO_3)_2^{2-}$ dimers.

Acknowledgment. The authors gratefully acknowledge the Wroclaw Supercomputer Center (WCSS) for providing computer time. We acknowledge the use of the Galera-ACTION Cluster and the support of The Academic Computer Center in Gdansk (CI TASK). The authors thank the Ministry of Science and the Higher Education of Poland (MNiSzW) for funding under grant no. N N204 0958 33. The authors thank Dr. Jaroslaw Panek and Dr. Rachel Glaves for fruitful discussion and comments.

References

(1) Madeja, F.; Havenith, M. *J. Chem. Phys.* **2002**, *117*, 7162–7168.

(2) Heyne, K.; Huse, N.; Nibbering, E. T. J.; Elsaesser, T. *Chem. Phys. Lett.* **2003**, *382*, 19–25.

(3) Heyne, H.; Huse, N.; Dreye, J.; Nibbering, E. T. J.; Elsaesser, T.; Mukamel, S. *J. Chem. Phys.* **2004**, *121*, 902–913.

(4) Nibbering, E. T. J.; Elsaesser, T. *Chem. Rev.* **2004**, *104*, 1887–1914.

(5) Ortlieb, M.; Havenith, M. *J. Phys. Chem.* **2007**, *A111*, 7355–7363.

(6) Miura, Y. S.; Tuckerman, M. E.; Klein, M. L. *J. Chem. Phys.* **1998**, *109*, 5290–5299.

(7) Ushiyama, H.; Takatsuka, H. *J. Chem. Phys.* **2001**, *115*, 5903–5912.

(8) Emmeluth, C.; Suhm, M. A.; Luckhaus, D. *J. Chem. Phys.* **2003**, *118*, 2242–2255.

(9) Durlak, P.; Morrison, C. A.; Middlemiss, D. S.; Latajka, Z. *J. Chem. Phys.* **2007**, *127*, 064304−064311.

(10) Dopieralski, P.; Panek, J.; Latajka, Z. *J. Chem. Phys.* **2009**, *130*, 164517164517−9.

(11) Kawaguchi, S.; Kitano, T.; Ito, K. *Macromolecules* **1992**, *25*, 1294–1299.

(12) Muller, B.; Schmelich, T. *Corros. Sci.* **1995**, *37*, 877–892.

(13) Wang, F. C.; Green, J. G.; Gerhart, B. B. *Anal. Chem.* **1996**, *68*, 2477–2481.

(14) Solich, M.; Krol, W.; Skirmuntt, K. *Pol. J. Chem.* **1993**, *67*, 433–443.

(15) James, M. N. G.; Williams, G. J. B. *Acta Crystallogr.* **1974**, *B30*, 1249–1257.

(16) Bednowitz, A. L.; Post, B. *Acta Crystallogr.* **1966**, *21*, 566–571.

(17) Wilson, C. C.; Shankland, N.; Florence, A. J. *Chem. Phys. Lett.* **1996**, *253*, 103–107.

(18) Thomas, J. O.; Tellgren, R.; Olovsson, I. *Acta Crystallogr.* **1974**, *B30*, 2540–2549.

(19) Macoas, E. M. S.; Fausto, R.; Lundell, J.; Pettersson, M.; Khriachtchev, L.; Rasanen, M. *J. Phys. Chem.* **2001**, *A105*, 3922–3933.

(20) Braun-Sand, S.; Olsson, M. H. M.; Mavri, J.; Warshel, A. Computer Simulation of Proton Transfer in Proteins and Solutions. In *Hydrogen Transfer Reactions*; Hynes, J. T., Klinman, J. P., Limbach, H.-H., Schowen, R. L., Eds.; Wiley-VCH Verlag GmbH: Weinhein, Germany, 2007; pp 1171−1205.

(21) Warshel, A. Calculations of Enzymic Reactions: Calculations of pKa, Proton Transfer Reactions, and General Acid Catalysis Reactions in Enzymes. *Biochemistry* **1981**, *20*, 3167.

(22) Warshel, A. Molecular Dynamics Simulations of Biological Reactions. *Acc. Chem. Res.* **2002**, *35*, 385–395.

(23) Kim, Y. *J. Am. Chem. Soc.* **1996**, *118*, 1522–1528.

(24) Dreyer, J. *Int. J. Quantum Chem.* **2005**, *104*, 782–793.

(25) Fernando-Ramos, A.; Smedarchina, A.; Rodriges-Otero, J. *J. Chem. Phys.* **2001**, *114*, 1567–1574.

(26) Stenger, J.; Madsen, D.; Dreyer, J.; Nibbering, E. T. J.; Hamm, P.; Elsaesser, T. *J. Phys. Chem.* **2001**, *A105*, 2929–2932.

(27) Car, R.; Parrinello, M. *Phys. Rev. Lett.* **1985**, *55*, 2471–2474.

(28) *CPMD*, version 3.11.1; IBM Research Division and Max Planck Institute: Stuttgart, Germany, 2008; www.cpmd.org.

(29) Gupta, M. P.; Mahata, A. P. *Indian J. Phys.* **1975**, *49*, 74–80.

(30) Shahat, M. *Acta Crystallogr.* **1952**, *5*, 763–768.

(31) Troullier, N.; Martins, J. L. *Phys. Rev.* **1991**, *B43*, 1993–2006.

(32) Perdew, J. P.; Burke, K.; Ernzerhof, M. *Phys. Rev. Lett.* **1996**, *77*, 3865–3868.

(33) Nose, S. *Mol. Phys.* **1984**, *52*, 255–268.

(34) Martyna, G. J.; Tuckerman, M. E.; Klein, M. L. *J. Chem. Phys.* **1992**, *97*, 2635–2643.

(35) Tuckerman, M. E. Path Integration via Molecular Dynamics. In *Quantum Simulation of Complex Many-Body Systems: From Theory to Algorithms*; Grotendorst, J., Marx, D., Muramatsu, A., Eds.; John von Neumann Institiute for Computing (NIC): Juelich, Germany, 2002, pp 269−298.

(36) Marx, D.; Parrinello, M. *Z. Phys.* **1994**, *B95*, 143–144.

(37) Marx, D.; Parrinello, M. *J. Chem. Phys.* **1996**, *104*, 4077–4082.

(38) Tuckerman, M. E.; Marx, D.; Klein, M. L.; Parrinello, M. *J. Chem. Phys.* **1996**, *104*, 5579–5588.

(39) Feynman, R. P.; Hibbs, A. R. *Quantum Mechanics, Path Integrals*; McGraw-Hill: New York, NY, 1965; pp 280−286.

(40) Schweizer, K. S.; Stratt, R. M.; Chandler, D.; Wolynes, P. G. *J. Chem. Phys.* **1981**, *75*, 1347–1363.

(41) Chandler, D.; Wolynes, P. G. *J. Chem. Phys.* **1981**, *74*, 4078–4095.

(42) Dopieralski, P.; Latajka, Z.; Olovsson, I. *Chem. Phys. Lett.* **2009**, *476*, 223–226.

(43) Forbert, H.;version 30.04.2002(harald.forbert@theochem.ruhr-uni-bochum.de) rev. A. Kohlmayer 04.05.2005, Lehrstuhl fuer Theoretische Chemie, Ruhr-University Bochum: Bochum, 2002.

(44) Ramirez, R. P.; Lopez-Ciudad, T.; Kumar, P.; Marx, D. *J. Chem. Phys.* **2004**, *121*, 3973–3983.

(45) Mathias, G.; Marx, D *Proc. Natl. Acad. Sci. U.S.A.* **2007**, *104*, 6980–6985.

(46) Kumar, P.; Marx, D. *Phys. Chem. Chem. Phys.* **2006**, *8*, 573–586.

(47) Rousseau, R.; Kleinschmidt, V.; Schmitt, U. W.; Marx, D. *Angew. Chem., Int. Ed.* **2004**, *43*, 4804–4807.

(48) Asvany, O.; Kumar, P.; Redlich, P. B.; Hegemann, I.; Schlemmer, S.; Marx, D. *Science* **2005**, *309*, 1219–1222.

(49) Humphrey, W.; Dalke, A.; Schulten, K. *J. Mol. Graphics* **1996**, *14*, 33–38.

(50) Zimmerli, U.; Parrinello, M.; Koumouutsakos, P. *J. Chem. Phys.* **2004**, *120*, 2693–2699.

(51) Steiner, T. *Angew. Chem.* **2002**, *41*, 48–76.

(52) Jeffrey, G. A. Nature and Properties. Strong hydrogen bonds. In *An Introduction to Hydrogen Bonding*; Oxford University Press: New York, NY, 1997; pp 11−55.

(53) Grotthuss, C. *Ann. Chim.* **1806**, *LVIII*, 54.

(54) Marx, D. *Chem. Phys. Chem.* **2006**, *7*, 1848–1870.

(55) Marechal, Y.; Witkowski, A. *J. Chem. Phys.* **1968**, *48*, 3697–3705.

(56) Marechal, Y. *J. Chem. Phys.* **1987**, *87*, 6344–6353.

(57) Bratos, S.; Hadzi, D. *J. Chem. Phys.* **1957**, *27*, 991–998.

(58) Chamma, D.; Henri-Rousseau, O. *Chem. Phys.* **1999**, *248*, 53–70.

(59) Chamma, D.; Henri-Rousseau, O. *Chem. Phys.* **1999**, *248*, 71–89.

(60) Dreyer, J. *J. Chem. Phys.* **2005**, *122*, 184306184306−10.

(61) Florio, G. M.; Zwier, T. S.; Myshakin, E. M.; Jordan, K. D.; Sibert, E. J., III *J. Chem. Phys.* **2003**, *118*, 1735–1746.

(62) Emmeluth, C.; Suhm, M. A. *Phys. Chem. Chem. Phys.* **2003**, *5*, 3094–3099.

(63) Chamma, D.; Henri-Rousseau, O. *Chem. Phys.* **1999**, *248*, 91–104.

(64) Bratos, S.; Leicknam, J.-Cl.; Gallot, G.; Ratajczak, H. Ultrafast Hydrogen Bonding Dynamics and Proton transfer Processes. In *The Condensed Phase*, Elsaesser, T., Bakkaer, H. J., Eds.; Kluwer Academic Publishers: Dordrecht, The Netherlands, 2002; pp 5.

(65) Giannopoulou, A.; Aletras, A. J.; Papatheodorou, G. N.; Yannopoulos, N. *J. Chem. Phys.* **2007**, *126*, 205101–205109.

(66) Stare, J.; Panek, J.; Eckert, J.; Grdadolnik, J.; Mavri, J.; Hadzi, D. *J. Phys. Chem. A* **2008**, *112*, 1576–1586.

(67) SDBSWeb; National Institute of Advanced Industrial Science and Technology: Tokyo, Japan; http://riodb01.ibase.aist.go.jp/sdbs/. Accessed July 19, 2009.

CT100078W